



A remote sensing-based dataset to characterize the ecosystem functioning and functional diversity in the Biosphere Reserve of Sierra Nevada (SE Spain)

5 Beatriz P. Cazorla^{1,2}, Javier Cabello^{1,2}, Andrés Reyes¹, Emilio Guirado^{1,3}, Julio Peñas^{1,4},
Antonio J. Pérez-Luque^{5,6}, Domingo Alcaraz-Segura^{1,4,5}

¹Andalusian Center for the Assessment and Monitoring of Global Change, University of Almería, 04120, Almería, Spain

²Department of Biology and Geology, University of Almería, 04120, Almería, Spain

³Multidisciplinary Institute for Environment Studies “Ramon Margalef” University of Alicante, 03690, Alicante, Spain

⁴Department of Botany, University of Granada, Av. de Fuentenueva, s/n 18071, Granada, Spain

10 ⁵icolab. Andalusian Institute for Earth System Research (IISTA-CEAMA) – University of Granada, Avda. Mediterráneo s/n,
E-18006, Granada, Spain.

⁶Terrestrial Ecology Research Group, Department of Ecology, Faculty of Science, University of Granada, Av. Fuentenueva
s/n, Granada, E-18071 Spain

Correspondence to: Beatriz P. Cazorla (b.cazorla@ual.es)

15

Abstract

Conservation Biology faces the challenge of safeguarding the ecosystem functions and ecological processes (water cycle, nutrients, energy flow, and community dynamics) that sustain the multiple facets of biodiversity. Characterization and evaluation of these processes and functions can be carried out through functional attributes or traits related to the exchanges of matter and energy between vegetation and the atmosphere. Based on this principle, satellite imagery can provide integrative spatiotemporal characterizations of ecosystem functions at local to global scales. Here, we provide a multi-temporal dataset at protected area level, that characterizes the spatial patterns and temporal dynamics of ecosystem functioning in the Biosphere Reserve of Sierra Nevada (Spain), captured through the spectral vegetation index EVI (Enhanced Vegetation Index, product MOD13Q1.006 from MODIS sensor) from 2001 to 2018. The database contains, at the annual scale, a synthetic map of Ecosystem Functional Types (EFTs) classes from three Ecosystem Functional Attributes (EFAs): i) descriptors of annual primary production, ii) seasonality, and iii) phenology of carbon gains. It also includes two ecosystem functional diversity indices derived from the above datasets: i) EFT richness, and ii) EFT rarity. Finally, it provides inter-annual summaries for all previous variables, i.e., their long-term means and inter-annual variabilities. The datasets are available in two open-source sites (PANGAEA: <https://doi.pangaea.de/10.1594/PANGAEA.924792> (Cazorla et al., 2020a) and http://obsnev.es/apps/efts_SN.html). This dataset brings to scientists, managers, and the general public, valuable information on the first characterization of ecosystem functional diversity based on primary production developed in Sierra Nevada, a biodiversity hotspot in the Mediterranean basin, and an

20
25
30
35



exceptional natural laboratory for ecological research within the Long-Term Social-Ecological Research (LTSER) network.

1 Introduction

40 A better characterization of the functional dimension of biodiversity is required to develop management approaches that ensure nature contributions to human well-being (Jax, 2010; Cabello et al., 2012a; Bennet et al., 2015). To achieve this goal is necessary a set of essential variables for characterizing and monitoring ecosystem functioning (Pereira et al., 2013). Such variables are critical to understanding the dynamics of ecological systems (Petchey and Gaston, 2006), the links between biological diversity and ecosystem services (Balvanera et al., 2006; Haines-Young and Potschin, 2010), and the mechanisms of ecological resilience (Mouchet et al., 2010). In addition, there have been calls for the use of ecosystem functioning variables to assess functional diversity at large scales to measure biosphere integrity (Mace et al., 2014; Steffen et al., 2015), one of the most challenging planetary boundaries to assess (Steffen et al., 2015). Despite the importance of ecosystem functioning variables and the conceptual frameworks developed to promote their use (Pettorelli et al., 2018), they have seldom been incorporated into ecosystem monitoring (see Alcaraz-Segura et al., 2009; Fernández et al., 2010; Cabello et al., 2016; Skidmore et al., 2021).

Characterization and evaluation of ecosystem functioning can be carried out through functional traits or attributes related to the matter and energy exchanges between biota and the atmosphere (Box et al., 1989; Running et al., 2000). Nowadays, the use of satellite imagery provides useful methods to derive such attributes, allowing for the spatially explicit characterization of ecosystem functioning and its heterogeneity (i.e., functional diversity) from local (Fernández et al., 2010) to regional (Alcaraz-Segura et al., 2006, 2013), and global scales (Ivits et al., 2013; Skidmore et al., 2021). Theoretical and empirical models support the relationship between spectral indices derived from satellite images (e.g., Enhanced Vegetation Index -EVI-) and essential functional variables of ecosystems, such as primary production, evapotranspiration, surface temperature, or albedo (Pettorelli et al., 2005; Fernández et al., 2010; Lee et al., 2013). Among them, primary production is one of the most integrative and essential descriptor of ecosystem functioning (Virginia and Wall, 2001; Pereira et al., 2013) since it has a central role in the carbon cycle (i.e., it is the energy input to the trophic web and therefore, the driving force behind many ecological processes) (Xiao et al., 2019). Moreover, primary production offers a holistic response to environmental changes and constitutes a synthetic indicator of ecosystem health (Costanza et al., 1992; Skidmore et al., 2015).

To characterize ecosystem functioning focusing on primary production, we can use the satellite-derived approach based on Ecosystem Functional Types (EFTs), defined as patches of the land surface that share similar dynamics in the matter and energy exchanges between the biota and the physical environment (Paruelo et al., 2001; Alcaraz-Segura et al., 2006). EFTs are derived from three Ecosystem Functional Attributes (EFAs) that describe the seasonal dynamics of carbon gains through time-series of spectral vegetation indices: 1) annual mean (a surrogate of annual primary production), 2) annual standard deviation (a descriptor of seasonality or the differences between the growing and non-growing seasons), and 3) the annual date of maximum (a phenological indicator of the date within a year on which the growing period is centered). Biologically, these three metrics can be interpreted as surrogates of the total amount and timing of primary production (Paruelo et al., 2001; Pettorelli et al., 2005; Alcaraz-Segura et al., 2006), one of the most integrative indicators of ecosystem functioning (Virginia and Wall, 2001). Since the EFT concept appeared in 2001 (Paruelo et al., 2001), its applicability has exponentially grown to characterize functional heterogeneity from local to global scales (Alcaraz-



80 Segura et al., 2006; Karlsen et al., 2006; Duro et al., 2007; Fernández et al., 2010; Geerken 2009; Alcaraz-Segura et al., 2013; Ivits et al., 2013; Cabello et al., 2013; Pérez-Hoyos et al., 2014; Müller et al., 2014; Wang and Huang, 2015; Villarreal et al., 2018; Coops et al., 2018; Mucina, 2019; Cazorla et al. 2020b).

85 Here, we present a dataset that describes the spatial heterogeneity and temporal variability of ecosystem functioning and ecosystem functional diversity patterns in a protected area. We derived the dataset from the analysis of the intra- and inter-annual variation of vegetation greenness captured through the EVI spectral vegetation index, as a surrogate of primary production, along the 2001-2018 period. As a case study, we used the Sierra Nevada Biosphere Reserve (SE Spain) (Fig. 1), a biodiversity hotspot in the Mediterranean basin and an exceptional natural laboratory for ecological research within the Long-Term Social-Ecological Research (LTSER) network. First, for each year, we provide three Ecosystem Functional Attributes (EFAs): i) annual primary production, and ii) seasonality and iii) phenology of carbon gains, as well as their integration into a synthetic mapping of Ecosystem Functional Types (EFTs) as discrete landscape functional units. Second, based on these units, we present two functional diversity metrics: EFT richness and EFT rarity. Finally, by considering the yearly maps, we calculated inter-annual summaries, i.e., inter-annual means and inter-annual variability, to show the average conditions and the stability of ecosystem functioning along the period (workflow in Fig. 2). The abundance of long-term datasets from multiple disciplines in Sierra Nevada constitutes an opportunity to explore the role of ecosystem functioning and functional diversity on ecohydrological and species distribution modeling, climate change mitigation and adaptation, ecological resilience, adaptive management, and ecosystem services supply.

2 Data description

2.1 Data acquisition and processing

105 We based ecosystem functioning characterization on analyzing the temporal dynamics of the Enhanced Vegetation Index (EVI) from 2001 to 2018. We chose EVI instead of any other vegetation index (such as SAVI, ARVI, or NDVI) as an indicator of carbon gains since it is more reliable in both low and high vegetation cover situations (Huete et al., 1997). EVI reduces the influence of atmospheric conditions on vegetation index values and corrects for canopy background signals.

EVI is computed following this equation (Equation 1):

$$EVI = G \times \frac{(NIR - RED)}{(NIR + C1 \times RED - C2 \times Blue + L)}$$

110 Equation 1, where NIR/RED/Blue are atmospherically-corrected (Rayleigh and ozone absorption) surface reflectances for near infrared, red and blue wavelengths, respectively; L is the canopy background adjustment that addresses the non-linear and differential transfer through a canopy of the NIR and red radiations; and C1, C2 are the coefficients of the aerosol resistance term, which uses the blue band to correct for aerosol influences in the red band. The coefficients adopted in the MODIS-EVI algorithm are; L=1, C1 = 6, C2 = 7.5, and G (gain factor) = 2.5. The EVI values range from -1 to +1, where negative values generally correspond to snow, ice, or water, and values closer to +1 represent the higher density of green leaves (Huete et al., 2002).



120 We obtained EVI from the MOD13Q1.006 product of the MODIS sensor (Moderate Resolution
Imaging Spectroradiometer) onboard NASA's Terra satellite (Didan, 2015). MOD13Q1.006 EVI
product is computed from atmospherically corrected bi-directional surface reflectances, by choosing
125 the best available pixel value from all the acquisitions (4 per day) in a 16-day period based on quality,
cloud presence, and viewing geometry (Huete et al., 1999; Didan et al., 2015). To further remove the
potential remaining effect of snow, ice, and water in our dataset, we transformed negative EVI values
into zeros. Thus, we obtained a maximum-value composite image every 16 days (23 images per year).
Despite its moderate spatial resolution (232 meters spatial resolution, though the nickname is 250 meters
pixel), we chose the MOD13Q1.006 product as the basis for our data since it offers a long time series
(almost 20 years) every 16 days, which allows for the characterization of the temporal dynamics of
130 ecosystem functioning (Anderson et al., 2018).

MOD13Q1.006 images are downloadable from NASA's LP DAAC (Land Processes Distributed Active
Archive Center) (<https://lpdaac.usgs.gov/products/mod13q1v006/>) (Didan, 2015). We processed them
through the Google Earth Engine (GEE) platform ([https://developers.google.com/earth-
135 engine/datasets/catalog/MODIS_006_MOD13Q1](https://developers.google.com/earth-engine/datasets/catalog/MODIS_006_MOD13Q1)). GEE combines a multi-petabyte catalog of satellite
imagery and geospatial datasets with planetary-scale analysis capabilities (Gorelick et al., 2017). We
used the main Javascript programming interface to build the algorithms and requests to GEE servers.
More information on <https://earthengine.google.com/faq/> and [https://developers.google.com/earth-
140 engine/](https://developers.google.com/earth-engine/). EVI values are multiplied by 10,000 to store them as real numbers to occupy less disk space
(both in the original MOD13Q1.006 product and in our dataset).

2.2 Calculating Ecosystem Functional Attributes (EFAs)

We calculated three EFAs known to capture most of the variance of the seasonal curve or annual
dynamics of vegetation indices (Paruelo et al., 2001; Alcaraz-Segura et al., 2006, 2009): the EVI annual
145 mean (EVI_mean; an estimator of primary production), the EVI seasonal Standard Deviation
(EVI_sSD; a descriptor of seasonality, i.e., the differences between the growing and non-growing
seasons), and the date of maximum EVI (EVI_DMAX; a phenological indicator of the month with
maximum EVI) (Fig. 3). To summarize the EFAs of the 2001-2018 period, we calculated the inter-
annual mean for each attribute (using linear statistics for EVI_mean and EVI_sSD and circular statistics
150 for EVI_DMAX).

To explore the robustness of these metrics in our study area, we examined their correlation with the first
axes of a Principal Component Analysis run on the EVI annual curve of the average year (i.e., 12 EVI
values corresponding to the inter-annual means of the 18 (one per year) maximum EVI values of each
155 month. These three metrics were highly correlated with the first two PCA axes (which accumulated
96.5% of variance), as previously reported for many regions (Townshend et al., 1985; Paruelo and
Lauenroth, 1998, Paruelo et al., 2001; Alcaraz-Segura et al., 2006, 2009; Ivits et al., 2013). See full
analysis in Supplement A.

160 2.3 Identifying Ecosystem Functional Types (EFTs)

EFTs were identified by dividing the EFAs into four intervals and combining them into a potential
number of 64 EFT classes ($4 \times 4 \times 4$), following a similar approach to Alcaraz-Segura et al., (2013)



(Figure 2). For EVI_DMAX, the four intervals agreed with the four seasons of the year: January to March = Winter, April to June = Spring, July to September = Summer, October to December = Autumn. For EVI_mean and EVI_sSD, we extracted the first, second, and third quartiles for each year. We verified that an 18-year period was long enough to stabilize the quartiles by running a sensibility analysis (see Supplement B). Then, for each quartile, we calculated the inter-annual mean of the 18-year period and used them as breaks between classes (Supplement B, Table S4). These breaks were applied back to each year as the thresholds for EVI_Mean and EVI_sSD to set EFT classes (Table 1). Finally, to summarize the EFTs, we calculated the most frequent EFT (i.e., the EFT mode for each pixel) of the 2001–2018 period. To name EFTs, we used two letters and a number: the first capital letter indicates primary production (EVI_mean), increasing from *A* to *D*; the second lower case letter represents seasonality (EVI_sSD), decreasing from *a* to *d*; finally, the numbers are a phenological indicator of the growing season (EVI_DMAX), with values *1-spring*, *2-summer*, *3-autumn*, *4-winter* (Table 1). The EFT alphanumeric code (*Aa1* to *Dd4*) corresponds to the numeric code (1 to 64) in the .TIF files, which is shown in the legend of Figure 4d.

2.4 Deriving Ecosystem Functional Diversity metrics

We derived two diversity metrics of ecosystem functional diversity from the EFT map: EFT richness and EFT rarity. EFT richness was calculated for each year by counting the number of different EFTs in a 4x4-pixel moving window around each pixel (top-left center pixel of a 4x4 kernel) (modified from Alcaraz-Segura et al., 2013). Each pixel received a richness value calculated by counting how many different EFTs there were in the surrounding 4x4 pixels. We chose a 4x4-pixel window since it offered the most acceptable spatial resolution without saturating the number of EFT classes per kernel (i.e., smaller kernel sizes resulted in a high proportion of moving windows saturated) (see sensitivity analysis on kernel size in section 3.2 and Supplement C).

We calculated EFT rarity as the extension of each EFT compared to the most abundant EFT in the study area (Equation 1) (Cabello et al., 2013). Then, the average rarity map of all years was obtained.

$$Rarity\ EFT_i = \frac{Area\ EFT_{max} - Area\ EFT_i}{Area\ EFT_{max}} \text{ (Equation 2)}$$

where $Area_EFT_{max}$ is the area occupied by the most abundant EFT, and $Area_EFT_i$ is the i EFT area being evaluated, with i ranging from 1 to 64.

Once we had the rarity value of each EFT (using Equation 2), we assigned to each pixel in the EFT map such value according to the pixel EFT class. Hence, the EFT rarity map spatial resolution was the same as the resolution of the EFT map (232 m).

2.5 Characterizing inter-annual stability in ecosystem functioning

We followed two approaches to characterize inter-annual stability of ecosystem functioning (either due to inter-annual fluctuations or directional trends). First, as an estimate of inter-annual variability of EFT occurrence at pixel level, we recorded the number of different EFTs that were observed at each pixel throughout the 2001–2018 period. Second, as an estimate of inter-annual dissimilarity of EFT composition at 4x4-pixel level, we started by calculating the dissimilarity (Equation 2) in the EFT composition of each 4x4-pixel window (924 x 924 m) between all possible combinations of two years



Then, we obtained the mean of the indices obtained from all possible combinations of years. We calculated dissimilarity as follows (Equation 3):

$$\text{Dissimilarity} = 1 - \text{Jaccard Index} \quad (\text{Equation 3})$$

205 where Jaccard similarity index is calculated as (Equations 4 and 5; Jaccard, 1901):

$$\text{Jaccard Index} = (\text{the number of shared classes between two sets}) / (\text{the total number of classes in either set}) * 100 \quad (\text{Equation 4})$$

The same formula in notation form is (Equation 5):

$$J(X, Y) = |X \cap Y| / |X \cup Y| \quad (\text{Equation 5})$$

210 This way, to calculate the Jaccard Index, we proceeded as follows: for each 4x4-pixel window, we first counted the number of EFTs shared between the two sets, i.e., the two years; second we counted the total number of EFTs that occurred in either set (shared and unshared between the two years); then, we divided the number of shared EFTs by the total number of EFTs; and finally, we multiplied the result by 100. Dissimilarity values ranged from 0 to 1, being 1 the highest degree of dissimilarity in EFT
215 composition throughout years, and 0 full similarity in EFT composition throughout years.

We processed inter-annual variability and inter-annual dissimilarity with IDL® software (Interactive Data Language). IDL is commonly used for interactive processing of large amounts of data, including image processing.

220 **3 Sensitivity and uncertainty analyses**

3.1 Effect of the EVI inter-annual variability on the boundaries set among EFT classes

To assess how inter-annual variability of EVI dynamics could affect the quartiles of EVI_Mean and EVI_sSD (which set the boundaries among EFT classes), we determined the minimum number of years needed in a study period to get stability in all quartiles (see Supplement B). For each quartile, we
225 plotted (Figure B1) the maximum inter-annual coefficient of variation observed across all possible combinations of consecutive years from 2001 to 2018 (i.e. from the 17 separate combinations of two consecutive years to a single combination of all 18 years together) against the number of years considered. Starting with two consecutive years, we plotted the maximum of 17 coefficients of variation (i.e., 2001-2002, 2002-2003, ... 2017-2018); for three consecutive years, the maximum of 16
230 coefficients of variation (i.e., 2001-2002-2003, ... 2016-2017-2018), and so on.

The inter-annual Coefficient of Variation (CV) of the 2001-2018 period was around 5% for the EVI_mean quartiles and around 10% for the EVI_sSD quartiles (Table B1, Supplement B). The quartiles of EVI_Mean (our surrogate for productivity) required at least 14 years to stabilize around
235 5% of CV. The quartiles of EVI_sSD (our surrogate for seasonality) required at least 17 years to stabilize around 10% of CV (Figure B1, Supplement B).

Despite the variation observed in the quartile values across years, we did not change the limits among EFT classes from one year to the next but instead applied the same limits to all years so we could
240 compare the classification output across years. That is, we followed a fixed-classification approach with



fixed limits among EFT classes for the entire period to make the classification able of detecting such inter-annual changes. For example, if a megawildfire burns the entire protected area in the future (e.g. in 2022), our use of fixed limits among classes for the 2001-2018 period will allow the detection of such disturbance (most pixels would be classified as low productivity "A EFT class"). Contrary, if the limits among EFT classes were adapted to the data distribution of each year, the classification would not detect the effect of wildfire on EVI dynamics and would impede the 2022 classification to be compared to previous years.

3.2 kernel size and borderline effect on EFT richness

To assess the effect of the size of the sliding window kernel on EFT richness and rarity, we calculated EFT richness for different kernel sizes (2x2, 3x3, 4x4, 5x5 pixels) and compared the outputs (see analysis in Supplement C). The 4x4-pixel kernel offered the most satisfactory spatial resolution of the EFT richness map without saturation of this variable (Figure C1, Supplement C). When the size of the sliding window kernels was 2x2 or 3x3 pixels, there was a high proportion of kernels that reached the highest possible richness value for that kernel size (i.e., 4 and 9 EFT classes per kernel, respectively), so the EFT richness variable was highly saturated. The 5x5-pixels kernel never reached the maximum number of pixels in a kernel but resulted in too coarse outputs (grain size of 5x5 MO13Q1 pixels, i.e., 1150x1150). Hence, the 4x4-pixel kernel offered a balance between output resolution and variable saturation, since we observed a maximum EFT richness of 13, while the maximum potential richness in a 4x4-pixel kernel was 16.

Pixels with NoData values were not considered a distinct class to compute EFT richness along the study area borderline. For these reason, it is important to note that the sliding windows along the borderline of the study area could systematically show lower EFT richness in our dataset than in reality.

4 Data structure and availability

Overall, the collection of datasets that we present here provides a characterization of ecosystem functioning and ecosystem functional diversity and inter-annual dynamics in Sierra Nevada Biosphere Reserve (SE Spain) derived from remote sensing. To broaden the use of data, we provided the datasets in two institutional scientific-repositories. Datasets are available for downloading in PANGAEA: <https://doi.pangaea.de/10.1594/PANGAEA.924792> (Cazorla et al., 2020a), and also at Sierra Nevada Global Change Observatory-LTER site, where we have also developed an *ad-hoc* visualization for the inter-annual summaries (http://obsnev.es/apps/efts_SN.html).

The dataset is structured in three main subsets of variables: Ecosystem Functional Attributes (EFAs), Ecosystem Functional Types (EFTs), and Ecosystem Functional Diversity (see Table 2). For each subset of variables, there are two groups of data (two subfolders): one containing the yearly variables, and another one containing the summaries for the 18-year period. A Data Management Plan with our dataset formal metadata is also available in PANGAEA data repository.

We provided the data in .TIF format and accompanied each .TIF file with a .TFW file containing its corresponding metadata. Additionally, we have also incorporated rendered versions of all layers as required by Google Earth Pro (called "filename..._forGoogleEarthVisualization.tif") for easing their visualization in this commonly used software. All data are available yearly (2001-2018) and summarized for the period. The spatial reference system of all data is EPSG:4326 Datum WGS84.



285 4.1 Data attribution

The MODIS database used in this work is maintained by NASA (satellite Terra, sensor MODIS, product MOD13Q1.006) and copied by Google into the Earth Engine servers (https://developers.google.com/earth-engine/datasets/catalog/MODIS_006_MOD13Q1). The Sierra Nevada Biosphere Reserve boundaries shapefile is included in the public official geodatabase of the Andalusian regional government (REDIAM: https://descargasrediam.cica.es/07_PATRIMONIO_NATURAL/01_ESPACIOS_PROTEGIDOS).

5 Data usage in Ecology and Conservation

295 Ecological research based on time series of spectral vegetation indices plays an essential role in biodiversity conservation (Cabello et al., 2012; Pettorelli, 2016, 2018) and management (Pelkey et al., 2003; Cabello et al., 2016), and for the study of biodiversity and ecosystems responses to environmental changes (Alcaraz-Segura et al., 2017; Pérez-Luque et al., 2015a, Skidmore et al., 2021). Recently, the use of EFAs derived from spectral vegetation indices in species distribution models has made possible to evaluate with high spatial and temporal precision habitat suitability for plant (Arenas-Castro et al., 300 2018) and animal species (Requena-Mullor et al., 2017; Regos et al., 2019) and may even anticipate expected changes in the distribution of threatened species as a consequence of climate change (Alcaraz-Segura et al., 2017). EFAs are also the basis of the monitoring program of the Spanish National Parks Network to identify changes and anomalies in ecosystem functioning, and to inform managers of ecosystem health and conservation status (Cabello et al., 2016).

305 Datasets based on an EFT approach can be useful for different purposes: to characterize spatial and temporal heterogeneity of ecosystem functioning from local to global scales (Alcaraz-Segura et al., 2006, Fernández et al., 2010, Cabello et al., 2013; Ivits et al., 2013); to evaluate the environmental and human controls of ecosystem functional diversity (Alcaraz-Segura et al., 2013); to identify priorities for Biodiversity Conservation (Cazorla et al., 2020b); to assess the representativeness of environmental 310 observatory networks (Villarreal et al., 2018); to assess the effects of land-use changes on ecosystem functioning (Oki et al., 2013); and to improve weather forecast models (Lee et al., 2013; Müller et al., 2014).

5.1 Case study

315 Sierra Nevada is a mountain range between 860 and 3482 *m a.s.l* covering more than 2000 km² in SE Spain (Fig. 1). It is one of the most critical biodiversity hotspots in the Mediterranean region (Blanca et al., 1998; Cañadas et al., 2014), hosting 105 endemic plant species and a total of 2353 taxa of vascular plants (33% and 20% of Spanish and European flora, respectively; Lorite 2016). Forest cover in Sierra Nevada is dominated by pine plantations covering approximately 40000 ha. The primary native forests are dominated by the evergreen holm oak *Quercus ilex* subsp. *ballota* (Desf.) Samp. 320 occupying low and medium mountain areas (8800 ha) and by the deciduous Pyrenean oak *Quercus pyrenaica* Willd. ranging from 1100 to 2000 *m a.s.l*. (about 2000 ha). Above the treeline, plant communities of the Oromediterranean and Crioromediterranean belts (above 1800-2000 *m a.s.l*), dominated by chamaephytes and hemicryptophytes (scrublands, grasslands, and cliff and scree communities), are the habitat to many endemisms.

325



Sierra Nevada receives legal protection and international recognition in multiple ways: UNESCO Biosphere Reserve (1986), Natural Park (1989), National Park (1999), Important Bird Area (2003), Special Area of Conservation in Natura 2000 network (2012), and it is in the IUCN Green List of Protected Areas (2014), a global standard of best practice for area-based conservation. Sierra Nevada is also a site within the European Long Term Ecological Research (LTER) network, with many available ecological data records from multiple disciplines (Zamora et al., 2017, LTER_EU_ES_010).

The dataset presented here provides the first characterization of functional diversity at ecosystem level for the Sierra Nevada Biosphere Reserve. Our dataset provides a baseline of ecosystem functioning for Sierra Nevada ecosystems, which opens the possibility to assess responses of ecosystem functioning to global change and management actions, to understand the drivers of ecosystem functioning and functional diversity, and to assess the supply of ecosystem services. This dataset provides valuable information for the Global Change Observatory of Sierra Nevada, a long-term ecological research site (name: ES- SNE, code: LTER_EU_ES_010) established more than a decade ago (Zamora et al., 2016, 2017), which is also now a mountain node of the LifeWatch ERIC (European Research Infrastructure Consortium). Thus, our dataset provides information at the level of ecosystem functioning that can be combined with other available datasets on this LTER site concerning on species distributions and dynamics, climate, ecosystem services, hydrology, land-use changes, and management practices (Pérez-Luque et al., 2014, 2015b, 2015c, 2016; Ros-Candeira et al., 2019, 2020; Lorite et al., 2020).

Results are briefly described in the following subsections:

345 **5.1.1 Ecosystem Functional Attributes spatial patterns**

Functional attributes of productivity, seasonality, and phenology showed a clear altitudinal pattern. Productivity (EVI_mean) was much lower above the treeline, i.e. in the high mountain bioclimatic belts (Cryoro- and Oromediterranean belts) than in lower belts (Supra- and Mesomediterranean belts). Productivity also decreased from west to east (Fig. 4a). Seasonality (EVI_sSD) was the highest in the Supramediterranean belt (Fig. 4b). Phenology (EVI_DMAX) was characterized by a dominant summer peak in vegetation greenness in the Cryoro- and Oromediterranean belts, and by a late spring peak in the Supra- and Mesomediterranean belts. Dry and semi-arid Thermomediterranean areas of the south and east showed greenness peaks in early autumn and winter months (Fig. 4c).

5.1.2 Ecosystem Functional Types map

355 As a result of the combination of the three Ecosystem Functional Attributes, productivity, seasonality, and phenology (Fig. 4 a-c), we obtained the EFT map (Fig. 4d). This map represents a synthetic characterization of ecosystem functioning spatial heterogeneity based on the primary production dynamics. A total of 64 EFTs classes were observed.

360 High-mountain areas (Cryoro- and Oromediterranean bioclimatic belts) showed EFTs with low and intermediate productivity, high seasonality, and maximum greenness in summer and spring. The extreme conditions of these areas, characterized by poor soils (Peinado et al., 2019), high solar radiation, extreme temperatures, winds, snow, and ice, constrain so much the vegetative period that they are known as "high-altitude cold desert" (Blanca et al., 2019). Mid-mountain areas (Supra- and Mesomediterranean belts) were associated with EFTs of intermediate-high productivity, medium-low seasonality, and maximum greenness in spring and autumn (e.g., Cc1-3) (Fig. 4d). The low dry and semi-arid areas (Thermomediterranean belts) of the south and east, characterized by thermophilic and



xerophytic species, displayed different EFTs to the rest of the park, with very low productivity, medium-low seasonality, and maximum greenness in spring or winter (e.g., Ac1-4).

5.1.3 Functional diversity at the ecosystem level

370 The highest EFT richness was observed in the Supra- and Mesomediterranean belts (Fig. 5c). Such
ecosystem functional diversity hotspots (i.e., EFT hotspots) could be related to two facts. First, many
Mediterranean mountains show high beta diversity (in terms of species turnover) around 1700-1900 m
a.s.l. (Wilson and Schmida, 1984), where there is a great structural and compositional replacement of
375 vegetation. Second, for the particular case of Sierra Nevada, in the mid-mountain and especially in its
southern face, there is a very diverse land cover mosaic, composed by different types of natural
vegetation (Valle et al., 2003), mixed with different types of pine afforestations, traditional croplands,
and land-uses (Camacho et al., 2002). The areas with the lowest EFT richness were located in Oro- and
Crioromediterranean belts, and in the eastern semi-arid Thermomediterranean extreme, where the harsh
soil and climatic conditions (Peinado et al., 2019) diminish floristic diversity (Fernández Calzado et al.,
380 2012).

EFT rarity was highest in the peaks (above 2800 m a.s.l., Cryoromediterranean belt) and the lowest
areas of the Eastern side of Sierra Nevada (semi-arid Thermomediterranean belt), both areas
characterized by a high concentration of narrowly endemic species (Mota et al., 2004; Cañadas et al.,
2014; Peñas et al., 2019). The high mountain areas (Oromediterranean belt) showed the lowest EFT
385 rarity, since their EFT composition was the most abundant and extensive in the Biosphere Reserve.
Mid-mountain areas (Supra- and Mesomediterranean belts) (Fig. 5d) showed medium to high EFT rarity
values. The relatively higher rarity of ecosystem functioning in these belts was associated with the
particular phenology of coniferous forests with autumn-winter maxima, also identified in other areas
of the Iberian Peninsula (Aragones et al., 2019).

390

5.1.4 Stability in the ecosystem functioning

The inter-annual variability ranged from 1 to 17 different EFTs over the 18-years period in the same
pixel (Fig. 5a). The inter-annual variability and inter-annual dissimilarity ($1 - \text{Jaccard index}$) (Fig. 5b)
395 observed was higher in the Supra- and Mesomediterranean levels, coinciding with the altitudinal range
where inter-annual climate variability is also higher (e.g., areas above the treeline are subjected to both
cold-snowy years and warm-dry years, Zamora et al., 2016). The eastern end of the semi-arid
Thermomediterranean areas also displayed a high inter-annual variability. There also exists significant
climate fluctuation in these areas, where small changes in the seasonal pattern of precipitation can
produce large changes in primary production (Houérou et al., 1988; Cabello et al., 2012b). On the other
400 hand, the most inter-annually stable areas (i.e. those that changed the least during the period) were
located in the Meso-Oromediterranean and Crioromediterranean belts, specifically, in the oak forests
and high-mountain meadows, ecosystems that are subjected to low human intervention.

6 Conclusion

405 We introduce a new dataset based on the processing and analysis of the temporal dynamics of the
Enhanced Vegetation Index (EVI) data from the MODIS sensor (MOD13Q1.006). The dataset contains



Ecosystem Functional Attributes (EFAs), Ecosystem Functional Types (EFTs), EFT richness, and EFT rarity in the Sierra Nevada Biosphere Reserve (SE Spain). EFAs represent functional attributes at the ecosystem level related to the primary production, seasonality, and phenology of carbon gains. EFTs are patches of the land surface that share similar dynamics in the exchanges of matter and energy between the biota and the physical environment, derived from the combination of the EFAs. EFT richness and EFT rarity are two metrics that inform on the spatial heterogeneity of primary production as focal ecosystem function. We also provide an estimation of the inter-annual stability of the former functional variables both at the pixel and at landscape levels throughout the 2001-2018 period. For this, we estimated the EFT inter-annual variability at each pixel and the inter-annual dissimilarity in the composition of EFTs at 4x4 sliding-window resolution. Overall, these data characterize the spatial and temporal patterns of ecosystem functioning and ecosystem functional diversity. The EFT approach adopted here improves our understanding of ecosystem processes and ecosystem response through environmental gradients. It provides scientists and managers valuable information to identify conservation priorities, assess ecosystem response to environmental changes, estimate ecosystem services provision, and to model species distributions and ecological and hydrological processes.

Author contributions

DAS, JC, JP and BPC designed the study, and DAS coordinated it. BPC and AR processed the images and produced the associated data sets presented in this paper. BPC prepared the manuscript with contributions from all authors. BPC and JC wrote the final version of the manuscript. BPC, EG, and AJPL prepared the final figures. AJPL designed and made the application to visualize the data. AJPL and BPC prepared the Data Management Plan. All authors reviewed the database and provided valuable feedback.

Competing interests. The authors declare that they have no conflict of interest.

Acknowledgements. BC was supported by the Plan Propio Ph.D. program of the University of Almería. E.G. is supported by the European Research Council grant agreement 647038 (BIODESERT). This research was developed as part of the projects: “Smart-EcoMountains” and “INDALO” (LifeWatch-2019-10-UGR-01 Ministerio de Ciencia e Innovación/Universidad de Granada/FEDER), partially funded by European Funds for Regional Development, “ECOPOTENTIAL: Improving future ecosystem benefits through earth observations” (<http://www.ecopotential-project.eu/>), which received funding from the European Union’s Horizon 2020 research and innovation program under grant agreement No 641762; Project “Ecosystem and Socio-Ecosystem Functional Types: Integrating biophysical and social functions to characterize and map the ecosystems of the Anthropocene” (CGL2014-61610-EXP), which received funding from the Spanish Ministry of Economy and Business; Project LIFE-ADAPTAMED (LIFE14 CCA/ES/000612): “Protection of key ecosystem services by adaptive management of Climate Change endangered Mediterranean socio-ecosystems”. E.G. was supported by the European Research Council grant agreement n° 647038 (BIODESERT). This research was done under the collaboration of the LTSER Platforms of the arid Iberian southeast, Spain, (LTER_EU_ES_027) and Sierra Nevada/Granada (ES- SNE), Spain (LTER_EU_ES_010), and contributes to the work done within the GEO BON working group on ecosystem function essential biodiversity variables.



References

450

Alcaraz-Segura, D., Paruelo, J. and Cabello, J.: Identification of current ecosystem functional types in the Iberian Peninsula, *Global Ecol and Biogeogr*, 15(2), 200–212, doi:10.1111/j.1466-822X.2006.00215.x, 395 2006.

455

Alcaraz-Segura, D., Cabello, J., Paruelo, J. M. and Delibes, M.: Use of Descriptors of Ecosystem Functioning for Monitoring a National Park Network: A Remote Sensing Approach, *Environ Manage.*, 43(1), 38–48, doi:10.1007/s00267-008-9154-y, 2009.

Alcaraz-Segura, D., Chuvieco, E., Epstein, H. E., Kasischke, E. S. and Trishchenko, A.: Debating the greening vs. browning of the North American boreal forest: differences between satellite datasets, *Global Change Biol*, 16(2), 760–770, 2010.

460

Alcaraz-Segura, D., Paruelo, J. M., Epstein, H. E. and Cabello, J.: Environmental and Human Controls of Ecosystem Functional Diversity in Temperate South America, *Remote Sens*, 5(1), 127–154, doi:10.3390/rs5010127, 2013.

Alcaraz-Segura, D., Lomba, A., Sousa-Silva, R., Nieto-Lugilde, D., Alves, P., Georges, D., Vicente, J. R. and Honrado, J. P.: Potential of satellite-derived Ecosystem Functional Attributes to anticipate species range shifts, *Int J of Appl Earth Obs*, 57, 86–92, doi:10.1016/j.jag.2016.12.009, 2017.

465

Anderson, C. B.: Biodiversity monitoring, earth observations and the ecology of scale. *Ecol Lett*, 21(10), 1572–1585, <https://doi.org/10.1111/ele.13106>, 2018.

Arenas-Castro, S., Gonçalves, J., Alves, P., Alcaraz-Segura, D. and Honrado, J. P.: Assessing the multi-scale predictive ability of Ecosystem Functional Attributes for species distribution modelling, *PLOS ONE*, 13(6), e0199292, doi:10.1371/journal.pone.0199292, 2018.

470

Balvanera, P., Pfisterer, A. B., Buchmann, N., He, J.-S., Nakashizuka, T., Raffaelli, D. and Schmid, B.: Quantifying the evidence for biodiversity effects on ecosystem functioning and services, *Ecol Lett*, 9(10), 1146–1156, doi:10.1111/j.1461-0248.2006.00963.x, 2006.

Blanca, G., Cueto, M., Martínez-Lirola, M. J. and Molero-Mesa, J.: Threatened vascular flora of Sierra Nevada (Southern Spain), *Biol Conserv*, 85(3), 269–285, doi:10.1016/S0006-3207(97)00169-9, 1998.

475

Blanca, G., Cueto, M. Romero A.T.: Rareza y endemidad en la flora vascular de Sierra Nevada, in *Biología de la conservación de plantas en Sierra Nevada: Principios y retos para su preservación*, pp. 325–343, Editorial Universidad de Granada, 2019.

480

Bennett, E.M., Cramer, W., Begossi, A., Cundill, G., Díaz, S., Egoh, B. N., ... and Lebel, L.: Linking biodiversity, ecosystem services, and human well-being: three challenges for designing research for sustainability. *Curr Opin Environ Sustain*, 14, 76–85, <https://doi.org/10.1016/j.cosust.2015.03.007>, 2015.

Box, E. O., Holben, B. N., and Kalb, V. Accuracy of the AVHRR vegetation index as a predictor of biomass, primary productivity and net CO₂ flux. *Vegetatio*, 80(2), 71–89, <https://doi.org/10.1007/BF00048034>, 1989.

485

Cabello, J., Fernández, N., Alcaraz-Segura, D., Oyonarte, C., Piñeiro, G., Altesor, A., Delibes, M. and Paruelo, J. M.: The ecosystem functioning dimension in conservation: insights from remote sensing, *Biodivers Conserv.*, 21(13), 3287–3305, doi:10.1007/s10531-012-0370-7, 2012a.



- Cabello, J., Alcaraz-Segura, D., Ferrero, R., Castro, A.J. & Liras, E. The role of vegetation and lithology in the spatial and inter-annual response of EVI to climate in drylands of Southeastern Spain. *Journal of Arid Environment*, 79, 76-83, 2012b
- 490 Cabello, J., Lourenço, P., Reyes-Díez, A. and Alcaraz-Segura, D.: Ecosystem services assessment of national parks networks for functional diversity and carbon conservation strategies using remote sensing, *Earth Observation of Ecosystem Services*, 179, 2013.
- Cabello, J., Alcaraz-Segura, D., Reyes-Díez, A., Lourenço, P., Requena-Mullor, J., Bonache, J., Castillo, P., Valencia, S., Naya, J., Ramírez, L. and Serrada, J.: Sistema para el Seguimiento del funcionamiento de ecosistemas en la Red de Parques Nacionales de España mediante Teledetección, *Revista de Teledetección*, 46, 119–131, doi:10.4995/raet.2016.5731, 2016.
- 495 Cabello, J., López-Rodríguez, M., Pacheco-Romero, M., Torres-García, M.T., Reyes-Díez, A.: Valores y argumentos para la conservación de la diversidad vegetal de Sierra Nevada, in *Biología de la conservación de plantas en Sierra Nevada: Principios y retos para su preservación*, pp. 345–361, Editorial Universidad de Granada., 2019.
- 500 Calzado, M. R. F., Mesa, J. M., Merzouki, A. and Porcel, M. C.: Vascular plant diversity and climate change in the upper zone of Sierra Nevada, Spain, *Plant Biosystems - Plant Biosystems*, 146(4), 1044–1053, doi:10.1080/11263504.2012.710273, 2012.
- Camacho-Olmedo, M., García-Martínez, P., Jiménez-Olivencia, Y., Menor-Toribio, J. and Paniza-Cabrera, A.: Dinámica evolutiva del paisaje vegetal de la Alta Alpujarra granadina en la segunda mitad del s. XX, *Cuad Geogr.*, 32(1), 25–42, 2002.
- Cañadas, E. M., Fenu, G., Peñas, J., Lorite, J., Mattana, E. and Bacchetta, G.: Hotspots within hotspots: Endemic plant richness, environmental drivers, and implications for conservation, *Biol Conserv*, 170, 282–291, doi:10.1016/j.biocon.2013.12.007, 2014.
- 510 Cazorla, B. P., Cabello, J., Peñas, J., Guirado, E., Reyes-Díez, A. and Alcaraz-Segura, D.: Funcionamiento de la vegetación y diversidad funcional de los ecosistemas de Sierra Nevada, in *Biología de la conservación de plantas en Sierra Nevada: Principios y retos para su preservación*, pp. 325–343, Editorial Universidad de Granada., 2019.
- 515 Cazorla, B. P., Cabello, J., Reyes-Díez, A., Guirado, E., Peñas, J., Pérez-Luque, A. J. and Alcaraz-Segura, D.: Ecosystem functioning and functional diversity of Sierra Nevada (SE Spain). University of Almería and Granada, PANGAEA, <https://doi.pangaea.de/10.1594/PANGAEA.924792>, 2020a.
- Cazorla, B. P., Cabello, J., Penas, J., Garcillan, P. P., Reyes, A. and Alcaraz-Segura, D.: Incorporating Ecosystem Functional Diversity into Geographic Conservation Priorities Using Remotely Sensed Ecosystem Functional Types. *Ecosystems*, 1-17. doi: <https://doi.org/10.1007/s10021-020-00533-4>, 2020b.
- 520 Coops, N. C., Kearney, S. P., Bolton, D. K. and Radeloff, V. C.: Remotely-sensed productivity clusters capture global biodiversity patterns, *Sci Rep*, 8(1), 16261, doi:10.1038/s41598-018-34162-8, 2018.
- Costanza, R., Norton, B. G. and Haskell, B. D.: *Ecosystem Health: New Goals for Environmental Management*, Island Press., 1992.



- 525 Didan, K.: MOD13Q1 MODIS/Terra vegetation indices 16-day L3 global 250m SIN grid V006, NASA 460 EOSDIS Land Processes DAAC, <https://doi.org/10.5067/MODIS/MOD13Q1.006>, 2015.
- Didan, K., Munoz, A. B., Solano, R., and Huete, A.: MODIS vegetation index user's guide (MOD13 series). University of Arizona: Vegetation Index and Phenology Lab, 2015.
- 530 Duro, D. C., Coops, N. C., Wulder, M. A. and Han, T.: Development of a large area biodiversity monitoring system driven by remote sensing, *Progress in Physical Geography: Earth Environ.*, 31(3), 235–260, doi:10.1177/0309133307079054, 2007.
- Fernández, N., Paruelo, J. M. and Delibes, M.: Ecosystem functioning of protected and altered Mediterranean environments: A remote sensing classification in Doñana, Spain, *Remote Sens Environ*, 114(1), 211–220, doi:10.1016/j.rse.2009.09.001, 2010.
- 535 Fernández Calzado, M. R., Molero Mesa, J., Merzouki, A., Casares Porcel, M.: Vascular plant diversity and climate change in the upper zone of Sierra Nevada, Spain. *Plant Biosystems-An Plan Biosystems*, 146(4),1044-1053, doi:<https://doi.org/10.1080/11263504.2012.710273>, 2012.
- Geerken, R. A.: An algorithm to classify and monitor seasonal variations in vegetation phenologies and their inter-annual change, *ISPRS J Photogramm*, 64(4), 422–431, doi:10.1016/j.isprsjprs.2009.03.001, 2009.
- 540 Gorelick, N., Hancher, M., Dixon, M., Ilyushchenko, S., Thau, D., and Moore, R.: Google Earth Engine: Planetary-scale geospatial analysis for everyone. *Remote Sens Environ*, 202, 18-27, <https://doi.org/10.1016/j.rse.2017.06.031>, 2017.
- Habitat Directive: Council Directive 92/43/EEC of 21 May 1992 on the conservation of natural habitats and of wild fauna and flora, *Official Journal of the European Union*, 206, 7–50, 1992.
- 545 Haines-Young, R. and Potschin, M.: The links between biodiversity, ecosystem services and human well-being, *Ecosyst Ecol: A New Synthesis*, doi:10.1017/CBO9780511750458.007, 2010.
- Huete, A. R., Liu, H. Q., Batchily, K. V., and Van Leeuwen, W. J. D. A.: A comparison of vegetation indices over a global set of TM images for EOS-MODIS. *Remote Sens Environ*, 59(3), 440–451, [https://doi.org/10.1016/S0034-4257\(96\)00112-5](https://doi.org/10.1016/S0034-4257(96)00112-5), 1997.
- 550 Huete, A., Justice, C., and Van Leeuwen, W.: MODIS vegetation index (MOD13). Algorithm theoretical basis document, 3(213), 1999.
- Huete, A., Didan, K., Miura, T., Rodriguez, E. P., Gao, X., and Ferreira, L. G.: Overview of the radiometric and biophysical performance of the MODIS vegetation indices. *Remote Sens Environ*, 83(1-2), 195–213, [https://doi.org/10.1016/S0034-4257\(02\)00096-2](https://doi.org/10.1016/S0034-4257(02)00096-2), 2002.
- 555 Ivits, E., Cherlet, M., Mehl, W. and Sommer, S.: Ecosystem functional units characterized by satellite observed phenology and productivity gradients: A case study for Europe, *Ecol Indic.*, 27, 17–28, doi:10.1016/j.ecolind.2012.11.010, 2013.
- Jaccard, P.: Étude comparative de la distribution florale dans une portion des Alpes et des Jura, *Bull Soc Vaudoise Sci Nat*, 37, 547–579, 1901.
- 560



Jax, K.: Ecosystem Functioning, Cambridge University Press, Cambridge., 2010.

Karlsen, S. R., Elvebakk, A., Høgda, K. A. and Johansen, B.: Satellite-based mapping of the growing season and bioclimatic zones in Fennoscandia, *Global Ecol Biogeogr*, 15(4), 416–430, doi:10.1111/j.1466-822X.2006.00234.x, 2006.

565 Le Houérou, H. N.: A probabilistic approach to assessing arid rangelands' productivity, carrying capacity and stocking rates, *Drylands: sustainable use of rangelands into the twenty-first century*, 159–172, 1998.

Lee, S.-J., Berbery, E. H. and Alcaraz-Segura, D.: The impact of ecosystem functional type changes on the La Plata Basin climate, *Adv. Atmos. Sci.*, 30(5), 1387–1405, doi:10.1007/s00376-012-2149-x, 2013.

570

Lorite, J.: An updated checklist of the vascular flora of Sierra Nevada (SE Spain), *Phytotaxa*, 261(1), 1–57, 2016.

Lorite, J., Ros-Candeira, A., Alcaraz-Segura, D., Salazar-Mendías, C.: FloraSNevada: a trait database of the vascular flora of Sierra Nevada, southeast Spain. *Ecology*. <https://doi.org/10.1002/ecy.3091>, Ecology, 2020.

575

Mace, G. M., Meyers, B., Alkemade, R., Biggs, R., Chapin, F. S., Cornell, S. E., Díaz, S., Jennings, S., Leadley, P., Mumby, P. J., Purvis, A., Scholes, R. J., Seddon, A. W. R., Solan, M., Steffen, W. and Woodward, G.: Approaches to defining a planetary boundary for biodiversity, *Global Env Chang*, 28, 289–297, doi:10.1016/j.gloenvcha.2014.07.009, 2014.

580 Mota, J. F., Sola, A. J., Jiménez-Sánchez, M. L., Pérez-García, F. and Merlo, M. E.: Gypsicolous flora, conservation and restoration of quarries in the southeast of the Iberian Peninsula, *Biodivers Conserv*, 13(10), 1797–1808, doi:10.1023/B:BIOC.0000035866.59091.e5, 2004.

Mouchet, M. A., Villéger, S., Mason, N. W. H. and Mouillot, D.: Functional diversity measures: an overview of their redundancy and their ability to discriminate community assembly rules, *Funct Ecol*, 24(4), 867–876, doi:10.1111/j.1365-2435.2010.01695.x, 2010.

585

Mucina, L.: Biome: evolution of a crucial ecological and biogeographical concept, *New Phytol*, 222(1), 97–114, doi:10.1111/nph.15609, 2019.

Müller, O. V., Berbery, E. H., Alcaraz-Segura, D. and Ek, M. B.: Regional Model Simulations of the 2008 Drought in Southern South America Using a Consistent Set of Land Surface Properties, *J. Climate*, 27(17), 6754–6778, doi:10.1175/JCLI-D-13-00463.1, 2014.

590

Oki, T., Blyth, E. M., Berbery, E. H. and Alcaraz-Segura, D.: Land Use and Land Cover Changes and Their Impacts on Hydroclimate, Ecosystems and Society, in *Climate Science for Serving Society: Research, Modeling and Prediction Priorities*, edited by G. R. Asrar and J. W. Hurrell, pp. 185–203, Springer Netherlands, Dordrecht., 2013.

595 Paruelo, J. M., and Lauenroth, W. K.: Regional patterns of normalized difference vegetation index in North American shrublands and grasslands. *Ecology*, 76(6), 1888–1898, <https://doi.org/10.2307/1940721>, 1995.



Paruelo, J. M., Jobbágy, E. G. and Sala, O. E.: Current Distribution of Ecosystem Functional Types in Temperate South America, *Ecosystems*, 4(7), 683–698, doi:10.1007/s10021-001-0037-9, 2001.

600 Peinado, F. J. M., Morales, M. N. J. and Ondoño, E. F.: Los suelos de Sierra Nevada, su relación con la litología y la vegetación, in *Biología de la conservación de plantas en Sierra Nevada: Principios y retos para su preservación*, pp. 173–192, Editorial Universidad de Granada., 2019.

Pelkey, N. W., Stoner, C. J. and Caro, T. M.: Assessing habitat protection regimes in Tanzania using AVHRR NDVI composites: Comparisons at different spatial and temporal scales, *Int J Remote Sens*, 24(12), 2533–2558, doi:10.1080/01431160210155929, 2003.

605 Peñas, J., Sánchez, E. C. and del Río Sánchez, J.: Fitogeografía de Sierra Nevada e implicaciones para la conservación, in *Biología de la conservación de plantas en Sierra Nevada: Principios y retos para su preservación*, pp. 81–116, Editorial Universidad de Granada., 2019.

Pereira, H. M., Ferrier, S., Walters, M., Geller, G. N., Jongman, R. H. G., Scholes, R. J., Bruford, M. W., Brummitt, N., Butchart, S. H. M., Cardoso, A. C., Coops, N. C., Dulloo, E., Faith, D. P., Freyhof, J., Gregory, 540 R. D., Heip, C., Höft, R., Hurr, G., Jetz, W., Karp, D. S., McGeoch, M. A., Obura, D., Onoda, Y., Pettorelli, N., Reyers, B., Sayre, R., Scharlemann, J. P. W., Stuart, S. N., Turak, E., Walpole, M. and Wegmann, M.: Essential Biodiversity Variables, *Science*, 339(6117), 277–278, doi:10.1126/science.1229931, 2013.

615 Pérez-Hoyos, A., Martínez, B., García-Haro, F. J., Moreno, Á. and Gilabert, M. A.: Identification of Ecosystem Functional Types from Coarse Resolution Imagery Using a Self-Organizing Map Approach: A Case Study for Spain, *Remote Sens*, 6(11), 11391–11419, doi:10.3390/rs61111391, 2014.

Pérez-Luque, A. J., Bonet, F. J., Pérez-Pérez, R., Aspizua, R., Lorite, J. and Zamora, R.: Sinfonevada: Dataset of floristic diversity in Sierra Nevada forests (SE Spain), *PhytoKeys*, 35, 1–15, doi:10.3897/phytokeys.35.6363, 2014.

Pérez-Luque, A. J., Pérez-Pérez, R., Bonet-García, F. J. and Magaña, P. J.: An ontological system based on MODIS images to assess ecosystem functioning of Natura 2000 habitats: A case study for *Quercus pyrenaica* forests, *Int J Appl Earth Obs*, 37, 142–151, doi:10.1016/j.jag.2014.09.003, 2015a.

Pérez-Luque, A. J., Zamora, R., Bonet, F. J. and Pérez-Pérez, R.: Dataset of MIGRAME Project (Global Change, Altitudinal Range Shift and Colonization of Degraded Habitats in Mediterranean Mountains), *PhytoKeys*, 56, 61–81, doi:10.3897/phytokeys.56.5482, 2015b.

Pérez-Luque, A. J., Sánchez-Rojas, C. P., Zamora, R., Pérez-Pérez, R. and Bonet, F. J.: Dataset of Phenology of Mediterranean high-mountain meadows flora (Sierra Nevada, Spain), *PhytoKeys*, 46, 89–107, doi:10.3897/phytokeys.46.9116, 2015c.

630 Pérez-Luque, A. J., Barea-Azcón, J. M., Álvarez-Ruiz, L., Bonet-García, F. J. and Zamora, R.: Dataset of Passerine bird communities in a Mediterranean high mountain (Sierra Nevada, Spain), *ZooKeys*, 552, 137–154, doi:10.3897/zookeys.552.6934, 2016.

Pérez-Luque, A. J., Bonet-García, F. J. and Zamora Rodríguez, R.: Map of ecosystems types in Sierra Nevada mountain (southern Spain). <https://doi.pangaea.de/10.1594/PANGAEA.910176>, 2019.



635 Petchey, O. L. and Gaston, K. J.: Functional diversity: back to basics and looking forward, *Ecology Letters*, 9(6), 741–758, doi:10.1111/j.1461-0248.2006.00924.x, 2006.

Pettorelli, N., Vik, J. O., Mysterud, A., Gaillard, J.-M., Tucker, C. J. and Stenseth, N. Chr.: Using the satellite-derived NDVI to assess ecological responses to environmental change, *Trends in Ecology & Evolution*, 20(9), 503–510, doi:10.1016/j.tree.2005.05.011, 2005.

640 Pettorelli, N., Wegmann, M., Skidmore, A., Múcher, S., Dawson, T. P., Fernandez, M., Lucas, R., Schaeppman, M. E., Wang, T., O'Connor, B., Jongman, R. H. G., Kempeneers, P., Sonnenschein, R., Leidner, A. K., Böhm, M., He, K. S., Nagendra, H., Dubois, G., Fatoyinbo, T., Hansen, M. C., Paganini, M., Klerk, H. M. de, Asner, G. P., Kerr, J. T., Estes, A. B., Schmeller, D. S., Heiden, U., Rocchini, D., Pereira, H. M., Turak, E., Fernandez, N., Lausch, A., Cho, M. A., Alcaraz-Segura, D., McGeoch, M.
645 A., Turner, W., Mueller, A., St-Louis, V., Penner, J., 560 Vihervaara, P., Belward, A., Reyers, B. and Geller, G. N.: Framing the concept of satellite remote sensing essential biodiversity variables: challenges and future directions, *Remote Sens Ecol Conserv*, 2(3), 122–131, doi:10.1002/rse2.15, 2016.

Pettorelli, N., Schulte to Bühne, H., Tulloch, A., Dubois, G., Macinnis-Ng, C., Queirós, A. M., Keith, D. A., Wegmann, M., Schrodte, F., Stellmes, M., Sonnenschein, R., Geller, G. N., Roy, S., Somers, B.,
650 Murray, N., Bland, L., Geijzendorffer, I., Kerr, J. T., Broszeit, S., Leitão, P. J., Duncan, C., Serafy, G. E., He, K. S., Blanchard, J. L., Lucas, R., Mairota, P., Webb, T. J. and Nicholson, E.: Satellite remote sensing of ecosystem functions: opportunities, challenges and way forward, *Remote Sens Ecol Conserv*, 4(2), 71–93, doi:10.1002/rse2.59, 2018.

Requena-Mullor, J. M., López, E., Castro, A. J., Alcaraz-Segura, D., Castro, H., Reyes, A. and Cabello, J.: Remote-sensing based approach to forecast habitat quality under climate change scenarios, *PLOS ONE*, 12(3), e0172107, doi:10.1371/journal.pone.0172107, 2017.

Ros-Candeira, A., Pérez-Luque, A. J., Suárez-Muñoz, M., Bonet-García, F. J., Hódar, J. A., Giménez de Azcárate, F. and Ortega-Díaz, E.: Dataset of occurrence and incidence of pine processionary moth in Andalusia, south Spain, *ZooKeys*, 852, 125–136, doi:10.3897/zookeys.852.28567, 2019.

660 Ros-Candeira, A., Moreno-Llorca, R., Alcaraz-Segura, D., Bonet-García, F.J., Vaz, A.S.: Social media photo content for Sierra Nevada: a dataset to support the assessment of cultural ecosystem services in protected areas. *Nat Conserv*, 38:1-12, 2020.

Running, S. W., Thornton, P. E., Nemani, R. and Glassy, J. M.: Global Terrestrial Gross and Net Primary Productivity from the Earth Observing System, in *Methods in Ecosystem Science*, edited by O. E. Sala, R. B. Jackson, H. A. Mooney, and R. W. Howarth, pp. 44–57, Springer New York, New York, NY., 2000.
665

Skidmore, A. K., Pettorelli, N., Coops, N. C., Geller, G. N., Hansen, M., Lucas, R., Múcher, C. A., O'Connor, B., Paganini, M., Pereira, H. M., Schaeppman, M. E., Turner, W., Wang, T. and Wegmann, M.: Environmental science: Agree on biodiversity metrics to track from space, *Nature*, 523(7561), 403–
670 405, doi:10.1038/523403a, 2015.

Skidmore, A. K., Coops, N. C., Neinavaz, E., Ali, A., Schaeppman, M. E., Paganini, M., ... & Wingate, V. Priority list of biodiversity metrics to observe from space. *Nature ecology & evolution*, 1-11, doi: 10.1038/s41559-021-01451-x, 2021.



675 Steffen, W., Richardson, K., Rockström, J., Cornell, S. E., Fetzer, I., Bennett, E. M., Biggs, R.,
Carpenter, S. R., Vries, W. de, Wit, C. A. de, Folke, C., Gerten, D., Heinke, J., Mace, G. M., Persson,
L. M., Ramanathan, V., Reyers, B. and Sörlin, S.: Planetary boundaries: Guiding human development
on a changing planet, *Science*, 347(6223), 1259855, doi:10.1126/science.1259855, 2015.

680 Townshend, J. R., Goff, T. E., and Tucker, C. J.: Multitemporal dimensionality of images of normalized
difference vegetation index at continental scales. *IEEE Trans Geosci Remote Sens*, (6), 888-895,
10.1109/TGRS.1985.289474, 1985.

Valle, F., Algarra, J. A., Arrojo, E., Asensi, A., Cabello, J., Cano, E., Cañadas Sánchez, E., Cueto, M.,
Dana, E. and Simón, D.: Mapa de series de vegetación de Andalucía, 2003.

685 Villarreal, S., Guevara, M., Alcaraz-Segura, D., Brunsell, N. A., Hayes, D., Loescher, H. W. and
Vargas, R.: Ecosystem functional diversity and the representativeness of environmental networks across
the conterminous United States, *Agr Forest Meteorol*, 262, 423–433,
doi:10.1016/j.agrformet.2018.07.016, 2018.

Virginia, R. A., Wall, D. H. and Levin, S. A.: Principles of ecosystem function, *Encyclopedia of
biodiversity*, 2, 345–352, 2001.

690 Wang, Y. and Huang, F.: Identification and analysis of ecosystem functional types in the west of
Songnen Plain, China, based on moderate resolution imaging spectroradiometer data, *JARS*, 9(1),
096096, doi:10.1117/1.JRS.9.096096, 2015.

Wilson, M. V. and Shmida, A.: Measuring beta diversity with presence-absence data, *J Ecol*, 1055–
1064, DOI: 10.2307/2259551, 1984.

695 Xiao, J., Chevallier, F., Gomez, C., Guanter, L., Hicke, J. A., Huete, A. R., ... and Sun, G. (2019).
Remote sensing of the terrestrial carbon cycle: A review of advances over 50 years. *Remote Sensing of
Environment*, 233, 111383.

Zamora Rodríguez, R. J., Pérez-Luque, A. J., Bonet, F. J., Barea-Azcón, J. M. and Aspizua, R.: Global
Change Impacts in Sierra Nevada: Challenges for Conservation. *Consejería de Medio Ambiente y
Ordenación del Territorio. Junta de Andalucía*. 208 pp, 2016.

700 Zamora, R., Pérez-Luque, A. J., Bonet, F. J., Barea-Azcón, J. M., Aspizua, R., Sánchez-Gutiérrez, F.
J., Cano-Manuel, F. J., Ramos-Losada, B. and Henares-Civantos, I.: Global Change Impact in the Sierra
Nevada Long-Term Ecological Research Site (Southern Spain), *The Bulletin of the Ecological Society
of America*, 98(2), 157–164, doi:[10.1002/bes2.1308](https://doi.org/10.1002/bes2.1308), 2017.

705

710



Figures

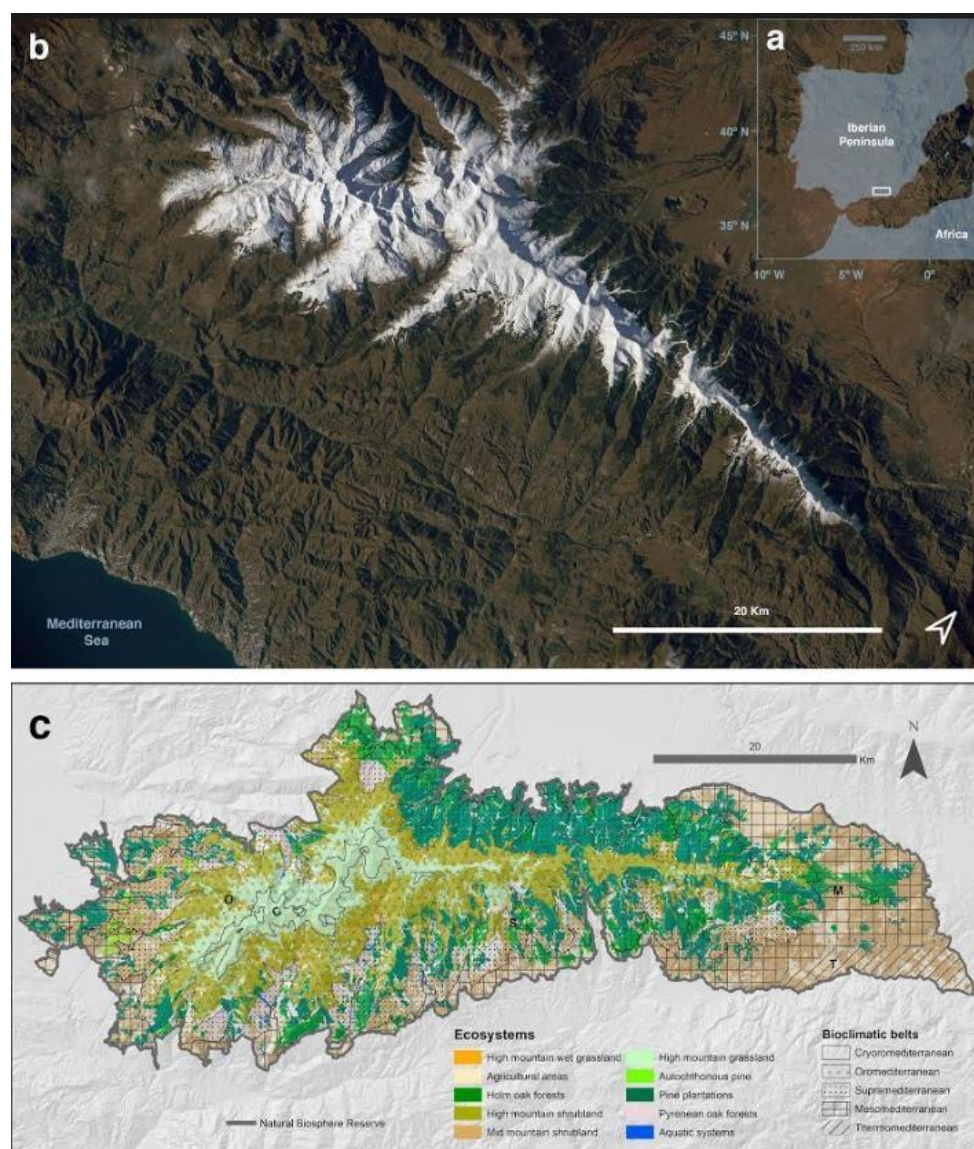
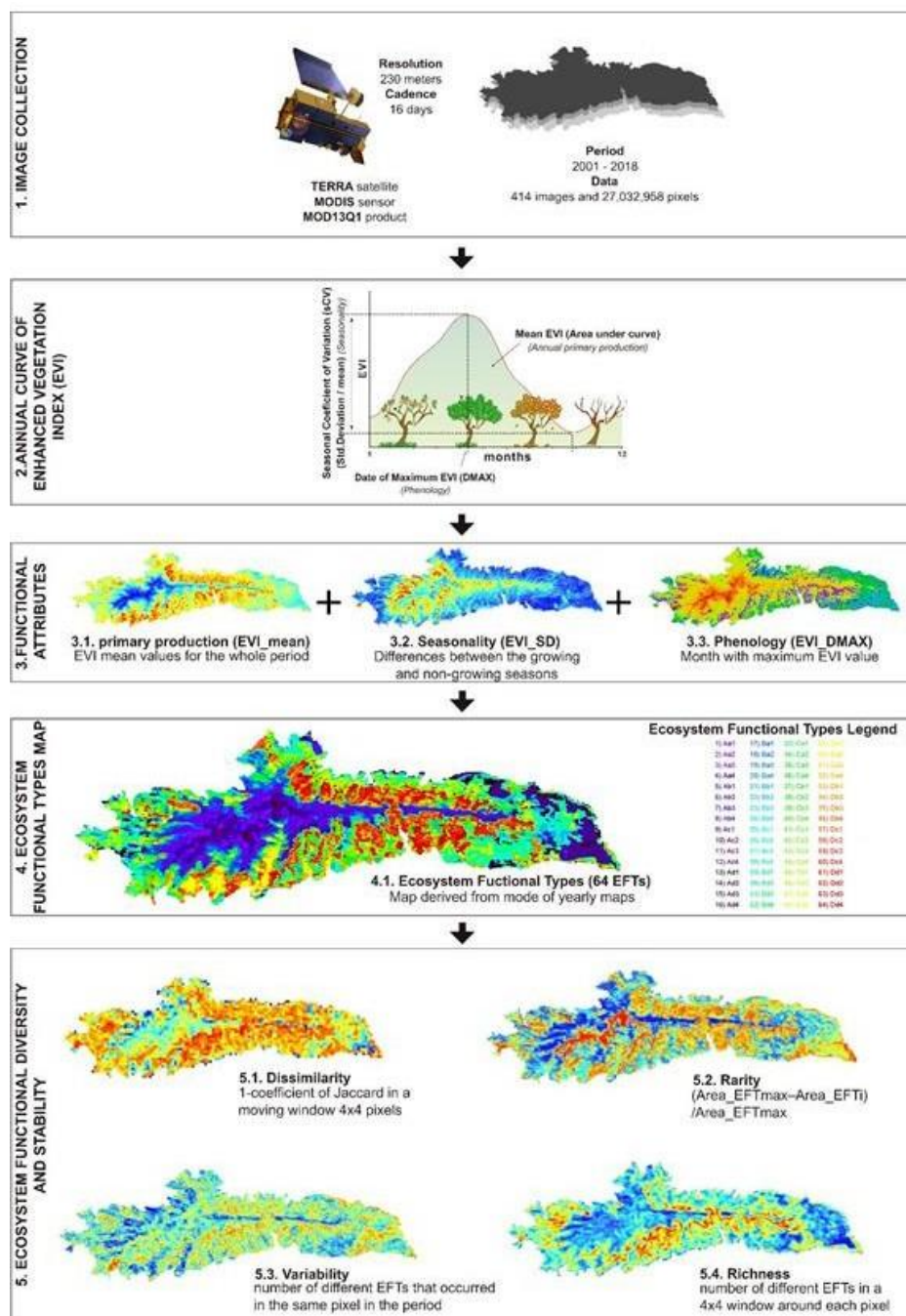


Figure 1. Study area: Sierra Nevada Biosphere Reserve. a) Location in the context of the Iberian Peninsula; b) remote view of Sierra Nevada mountain region (image from the International Space Station took in December 2014; courtesy of “Earth Science and Remote Sensing Unit, 615 NASA Johnson Space Center”); c) delimitation of the Biosphere Reserve and the distribution of the main ecosystems (Pérez-Luque et al., 2019) and thermotype bioclimatic belts (Molero-Mesa and Marfil, 2015).

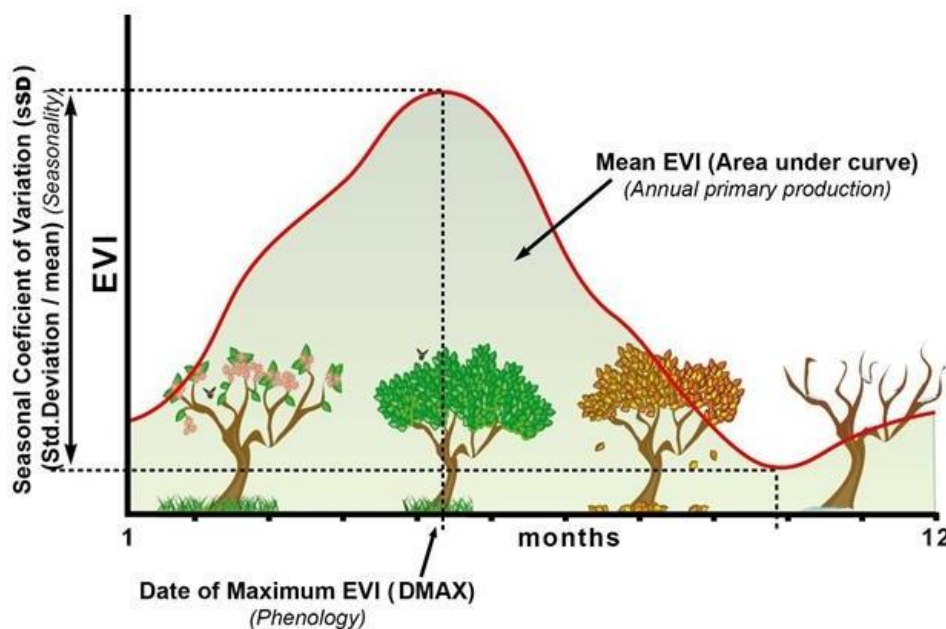


720 **Figure 2.** Workflow to characterize the ecosystem functioning and functional diversity of Sierra Nevada. MODIS (Moderate Resolution Imaging Spectroradiometer) sensor product MOD13Q1 onboard NASA's Terra satellite was used. This product contains maximum value composite images with 16-day temporal resolution (23 images per year) and 232 m spatial resolution for the Enhanced Vegetation Index (EVI) (1).



725

The study period was from 2001 to 2018. Three ecosystem functional attributes (EFAs) describing ecosystem functioning were calculated from the EVI seasonal curve for each year (2 and 3). The range of values for each attribute was divided into four intervals, resulting in a potential number of 64 ecosystem functional types (EFTs; $4 \times 4 \times 4 = 64$) (4). From EFTs, we derived four metrics related to ecosystem functional diversity (i.e., EFT richness and rarity) and ecosystem functional stability (i.e., inter-annual variability and dissimilarity) (5).

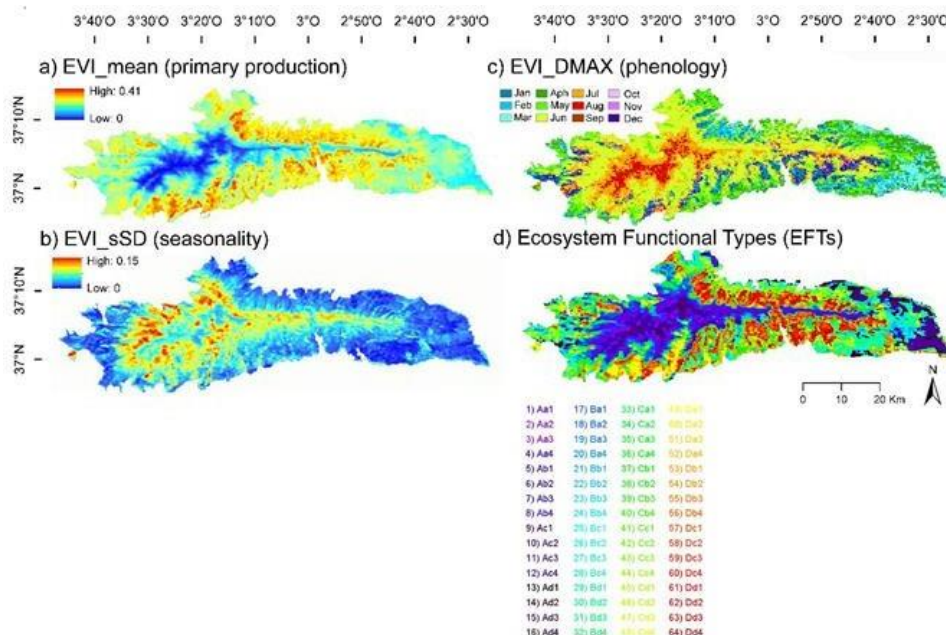


730

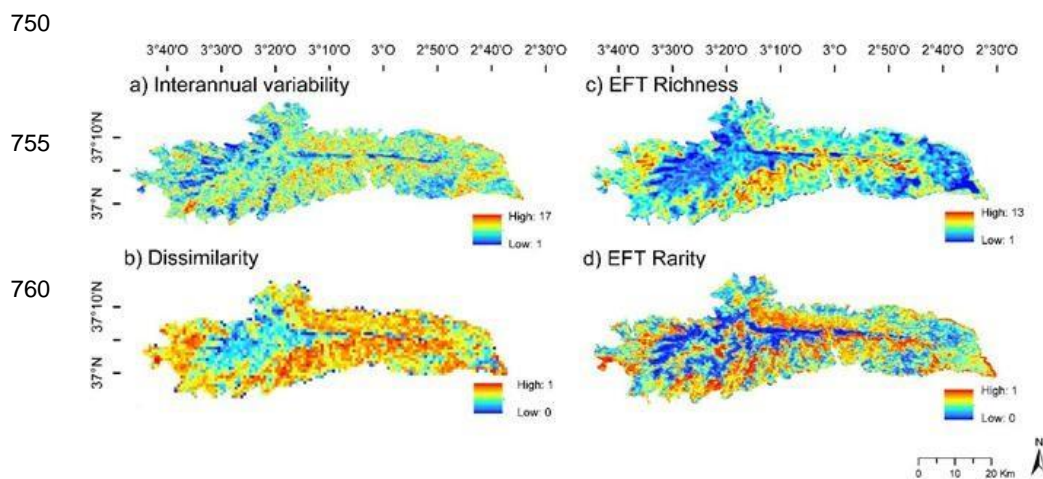
Figure 3: Seasonal dynamics of Enhanced Vegetation Index (EVI) and EVI derived metrics or Ecosystem Functional Attributes (EFAs). The “X” axis corresponds to the months of the year and the “Y” axis to the EVI values. EFAs were: the annual mean of EVI, an estimator of annual primary production (EVI_mean); the EVI seasonal coefficient of variation, i.e. a descriptor of seasonality or the differences between the growing and non growing seasons (EVI_sSD), and the date of maximum EVI, a phenological indicator of the growing season (EVI_DMAX). We chose these three EVI metrics or EFAs since they capture most of

735

the variance (96.5%) of the EVI seasonal dynamics in a Principal Component Analysis.



740 **Figure 4.** Ecosystem Functional Attributes (EFAs; a-c) and Ecosystem Functional Types (d) describing the
 functioning of vegetation canopy based on the Enhanced Vegetation Index (EVI), derived from MOD13Q1-
 TERRA (pixel 232 m) for the period 2001-2018. EFAs were (a-c): the annual mean of EVI, an estimator of
 annual primary production (EVI_mean); the EVI seasonal coefficient of variation, i.e. a descriptor of
 seasonality or the differences between the growing and non growing seasons (EVI_sSD), and the date of
 maximum EVI, a phenological indicator of the growing season (EVI_DMAX). To name EFTs (d), we used
 745 two letters and a number: the first capital letter indicates primary production (EVI_mean), increasing from
 A to D; the second lower case letter represents seasonality (EVI_sSD), decreasing from a to d; finally, the
 numbers are a phenological indicator of the growing season (EVI_DMAX), with values 1-spring, 2-summer,
 3-autumn, 4-winter (Table 1). The EFT alphanumeric code (Aa1 to Dd4) corresponds to the numeric code
 (1 to 64) in the .TIF files, as shown in the panel legend (d).



750
755
760
765
770

Figure 5. Functional diversity and stability patterns based on the identification of ecosystem functional types (EFTs) derived from Enhanced Vegetation Index (EVI) images captured by MOD13Q1-TERRA sensor along the 2001-2018 period. a) EFT inter-annual variability for the period, i.e., number of EFTs that occurred at each pixel throughout the period; b) EFT inter-annual dissimilarity (1 - Jaccard index), i.e., mean inter-annual dissimilarity of EFT composition in 4x4 MODIS-pixel windows between all possible combinations of pairs of years throughout the period; c) Spatial EFT richness patterns, i.e., number of different EFTs observed in a 4x4 MODIS-pixel sliding window ($\sim 232\text{m} \times 4 = \sim 1\text{ km}^2$); and d) Spatial EFT rarity patterns, i.e., a measure of the relative scarcity or abundance of each EFT in the study area.



775 **Table 1. Ecosystem functional attribute (EFA) ranges used for the identification of ecosystem functional**
types (EFTs) in the Sierra Nevada Biosphere Reserve. For EVI_DMAX, the four intervals agree with the
four seasons of the year. For EVI_mean and EVI_sSD, we extracted the first, second, and third quartiles
for each year and then calculated the inter-annual mean of each quartile (their average over the 18-year
period). The values of both EVI_mean and EVI_sSD are multiplied by 10,000 in the .TIF files to save disk
780 **space.**

Ecosystem Functional Attribute	EFT Character code	Digit code	Range
EVI Mean (Productivity)	A	100	0 - 0.137
	B	200	0.137 - 0.187
	C	300	0.187 – 0.241
	D	400	> 0.241
EVI sSD (Seasonality)	a	10	> 0.062
	b	20	0.043 – 0.062
	c	30	0.030 – 0.043
	d	40	0 – 0.030
EVI DMAX (Phenology)	1	1	Spring
	2	2	Summer
	3	3	Autumn
	4	4	Winter

785



Table 2. Dataset description: Ecosystem Functional Attributes (EVI_Mean, EVI_sSD and EVI_MMAX provided yearly and summarized for the 2001-2018 period as inter-annual mean); Ecosystem Functional Types (EFTs provided yearly and summarized for the period as inter-annual mode, variability and dissimilarity); Ecosystem Functional Diversity (EFT richness and EFT rarity, provided yearly and summarized for the period as inter-annual mean). Spatial resolution is ~231 in all cases except in the EFT dissimilarity, where it is ~232m x 4 = ~1km². YYYY refers to year and varies from 2001 to 2018.

Filename	Variable	Definition	Biological significance	Temporal resolution
EVI_Mean_YYYY_C006_MOD13Q1_Pixel232	EVI_mean	Mean of the positive EVI values in a year	Primary production in a year	Yearly, one image per year YYYY
EVI_Mean_InterAnnualMean_2001-2018_C006_MOD13Q1_Pixel232	EVI_mean	Inter-annual mean of the annual EVI_mean values of the period	Average annual primary production of the period	One image for the 2001-2018 period
EVI_sSD_YYYY_C006_MOD13Q1_Pixel232	EVI_sSD	Intra-annual standard deviation of the positive EVI values within a year	Seasonality in vegetation greenness. Differences in carbon gains between the growing and non-growing seasons in a year	Yearly, one image per year YYYY
EVI_sSD_InterannualMean_2001-2018_C006_MOD13Q1_Pixel232	EVI_sSD	Inter-annual mean of the annual EVI_sSD values of a period	Seasonality. Average difference in carbon gains between the growing and non-growing seasons throughout the period	Average of the 2001-2018 period
EVI_MMAX_YYYY_C006_MOD13Q1_Pixel232	EVI_DMAX	Month with maximum EVI in a year	Phenology. Month of maximum greenness in a year	Yearly, one image per year YYYY
EVI_MMAX_InterannualMean_2001-2018_C006_MOD13Q1_Pixel232	EVI_DMAX	Inter-annual mean of the month with maximum EVI of the period	Phenology. Average month with maximum greenness throughout the period	Average of the 2001-2018 period
EFTs_YYYY_C006_MOD13Q1_Pixel232	EFTs	Range of EFA's values divided into four intervals $4 \times 4 \times 4 = 64$ potential EFTs in a year	Patches of land surface that share similar dynamics in matter and energy exchanges in a year	Yearly, one image per year YYYY
EFTs_InterannualMode_2001-2018_C006_MOD13Q1_Pixel232	EFTs	Mode of the range of EFA's values divided into four intervals $4 \times 4 \times 4 = 64$ potential EFTs of the period	Patches of land surface that share similar dynamics in matter and energy exchanges throughout the period	Mode of the 2001-2018 period



EFT_InterannualVariability_2001-2018_C006_MOD13Q1_Pixel232	EFT interannual variability	N° of different EFTs that occurred in the same pixel in the period	Inter-annual changes in ecosystem functioning throughout the period at pixel level	2001-2018 period
EFT_InterannualDissimilarity_2001-2018_C006_MOD13Q1_Pixel232	EFT interannual dissimilarity	1 - <i>Jaccard Index</i>	Inter-annual changes in EFT composition throughout the period at 4x4 MODIS-pixel level	2001-2018 period
EFT_Richness_YY_C006_MOD13Q1_Pixel232	EFT richness	N° of different EFTs in a 4x4-pixel moving window around each pixel in a year	Spatial heterogeneity in EFT composition in each year in 4x4 MODIS-pixel kernels	Yearly, one image per year YYYY
EFT_Richness_InterannualMean_2001-2018_C006_MOD13Q1_Pixel232	EFT richness	N° of different EFTs in a 4x4-pixel moving window (924 x 924 m) around each pixel in a period	Average spatial heterogeneity in EFT composition throughout the period in 4x4 MODIS-pixel kernels	Average of the 2001-2018 period
EFT_Rarity_YYYY_C006_MOD13Q1_Pixel232	EFT rarity	$Rarity\ of\ EFT_i = (Area_EFT_{max} - Area_EFT_i) / Area_EFT_{max}$ (in a year)	EFT geographical scarcity or abundance in the study area in each year	Yearly, one image per year YYYY
EFT_Rarity_InterannualMean_2001-2018_C006_MOD13Q1_Pixel232	EFT rarity	$Rarity\ of\ EFT_i = (Area_EFT_{max} - Area_EFT_i) / Area_EFT_{max}$ (in a period)	Average EFT geographical scarcity or abundance in the study area throughout the period	Average of the 2001-2018 period